

## POLARIZATION OF THE RELATIVISTIC JET OF PKS1136-135

J. S. NIEDZIELSKI

Department of Physics and Astronomy, Michigan State University, East Lansing, MI 48823

AND

E.S. PERLMAN

Department of Physics and Space Sciences, Florida Institute of Technology, Melbourne, FL 32901

### ABSTRACT

A prominent feature of many active galaxies is their relativistic jets. These jets emerge from the nucleus at speeds up to 99.9% of  $c$  and carry energy from the central regions out to distances of hundreds of kiloparsecs. The jets are composed of high-energy plasma that is known to emit via the synchrotron mechanism at radio through infrared energies. However, the emission mechanism is not well constrained at optical through X-ray energies, particularly for the most powerful jets, those located in luminous quasars. Multi-waveband observations of a few quasar jets have recently found that a common emission component connects the optical through X-ray bands. In these objects, optical polarimetry provides a powerful test for both the X-ray and optical emission mechanisms. Here we discuss imaging polarimetry of the jet of PKS 1136-135, a luminous quasar at  $z = 0.554$ , obtained with the Hubble Space Telescope. Our results show that different mechanisms dominate in the optical and X-rays for different regions of the jet. Knot A is highly polarized and so its optical and X-ray emission must be due to synchrotron radiation. However no significant polarization is detected in any other jet component, strongly indicating inverse-Comptonization of Cosmic Microwave Background photons as the optical-X-ray emission mechanism. The low polarization also independently rules out synchrotron self-Compton as the X-ray production mechanism in a model-independent way.

*Subject headings:* Quasars: individual (PKS 1136-135), Galaxies: active, Galaxies: jets, Techniques: polarimetric

### 1. INTRODUCTION

One of the most interesting features in extra-galactic astronomy is that of the relativistic jet of charged particles that is observed in most active galaxies. PKS1136-135 is an active galaxy that contains one of these relativistic jets. PKS1136-135 is located in the constellation Crater. It is a quasar with a high luminosity. With a redshift of  $z = 0.554$ , PKS1136-135 is relatively close for a quasar. As a result, observations of this object can yield somewhat better linear resolution than those of other, more distant quasars. The structure of the jet of PKS1136-135 is resolved well in several bands, including X-ray, optical, mid-infrared and radio (Sambruna et al. 2002; Uchiyama et al. 2007). (Uchiyama et al. 2007) analyzed the multiwaveband spectrum of the jet, showing that a single power-law emission component connected the emission in the optical and X-ray for the two brightest knots.

For the radio to optical bands it is widely agreed that the emission mechanism in relativistic jets is synchrotron radiation. The main reason behind this is the high polarization observed in the radio band, which precludes thermal mechanisms. In addition, the radiation in the infrared and optical usually has an overall power-law shape that can be smoothly connected to the radio emission (Harris & Krawczynski 2006). Synchrotron radiation emanates from high energy charged particles that gyrate within in a magnetic field (Longair, p.101 1992). The synchrotron radiation can be produced either by highly energetic electrons or protons. Regardless of which synchrotron subspecies the emission may be, we know we

should observe significant polarization.

At higher energies, the radiation mechanism is strongly debated, with both inverse-Compton and synchrotron emission being viable models. In lower-power objects (FR I radio galaxies), it is believed that the synchrotron mechanism dominates up to X-ray energies, but in more powerful jets (FR II radio galaxies and quasars) the optical emission often falls well below an extrapolation of radio through X-rays, making synchrotron emission models more difficult. For those objects it is believed that inverse-Compton emission plays an increasingly important role in the X-rays, perhaps amplified by relativistic beaming. In inverse-Compton (IC) scattering, high energy photons scatter lower-energy photons. The lower energy photons gain energy, and thus the Compton scattering is 'inversed' (Longair, p.229 1994). The seed photons can originate in a variety of places, including the jet itself (the synchrotron self-Compton or SSC mechanism), other AGN regions, as well as the Cosmic Microwave Background (CMB).

Because of the controversy over the high-energy emission mechanism, it is important to find diagnostics to discriminate between the models. Polarimetry stands out as a diagnostic, because the emission from the CMB is not polarized, and as a result, inverse-Compton scattered CMB (IC-CMB) emission also should not be polarized (Uchiyama et al. 2007). By comparison, high polarization is expected in the synchrotron and SSC mechanisms. Polarimetry is also useful as the electric vector of synchrotron emission should be aligned at 90 degrees from the direction of the magnetic field, and is therefore a direction diagnostic of the field structure in the emis-

sion region, and is thus a much more useful diagnostic than standard imagery, which can be fooled quite easily by simple superposition. With polarimetry, however, superposition is much more difficult as the vectors would also have to cancel. A downside to polarimetry is the difficulty in data processing and reduction, as well as the fact that the observing requirements are rather extreme.

Recent observations have shown that in some jets, notably those of PKS1136-135 and 3C 273, the X-ray and optical emission are connected by a single component (Uchiyama et al. 2007; Jester et al. 2006; ?). In these objects, optical polarimetry can thus serve as a powerful diagnostic of the emission mechanism not only in the optical but also in the X-rays. It was for this reason that we decided to observe the jet of PKS1136-135 in the optical with the Hubble Space Telescope (HST). X-ray polarimetry is beyond the capabilities of current instruments and so these observations give us unique information.

## 2. OBSERVATIONS

We observed the jet of PKS1136-135, using the Hubble Space Telescope with the POLQ polarization filter and the F555W optical filter, to identify if the knot features located within the relativistic jet of PKS 1136-135 showed significant polarization. A total of 21 orbits split up into 6 visits were used to observe the source with the Hubble Space Telescope. The 555 nanometer wavelength shows good characteristics for polarization. At this wavelength we get a maximum of parallel polarized radiation, while getting a minimum of perpendicular polarized radiation. Therefore, this band is best suited for polarimetry. The data was reduced using various tasks in IRAF and AIPS. Once Stokes images and their associated error images were obtained, an analysis of the result was conducted.

All observations were conducted via the Hubble Space Telescope. A total of 21 orbits were taken on PKS 1136-135; the most detailed optical observation of this source to date. The observing run was split up into 6 different visits; 50, 51, 60, 61, 70, and 71. Visits 50, 60, and 70 all had four exposures of 2500 seconds. Visits 51, 61, and 71 had three exposures of 2500 seconds. The Wide Field and Planetary camera 2 (WFPC-2) was used for the observations. Traditionally the Advanced Camera for Surveys (ACS) would have been used in an extragalactic observation such as this, but due to electronic problems the ACS was not available when the proposed observations were conducted.

WFPC-2 is a combination wide-field and planetary camera that is very flexible. It is split up into three wide field (WF) CCD detectors and a single planetary chip (PC) CCD detector. While all 4 CCD detector chips of WFPC-2 were used, (WF2, WF3, WF4, and PC), PKS 1136-135 and its associated jet were only located on the WF2, WF3, or WF4 chip of the detector, depending on the visit. Visits 50 and 51 had the target in the WF2 chip, visits 60 and 61 had the target in the WF3 chip, and visits 70 and 71 had the target in the WF4 chip. In all visits, the orientation of the HST was constrained to be the same. The reason for this strategy was so that three polarization angles, differing by 0, 45 and 90 degrees, could be obtained. The POLQ filter is actually four filters in a quad pattern, with only limited rotational ability. Thus the easiest way to obtain the necessary data

is to observe through each of the three WF chips.

X-ray data from the Chandra X-ray observatory, observed on 16 April, 2003 by Sambruna et al. (2002), was used for comparison. An X-ray image sub-sampled by 0.5 was taken from ACIS on Chandra was overlaid with the Polarization intensity image. A .65 arc second resolution radio image from the Very Large Array, provided by C. C. Cheung, was also used for comparison. The radio image is in the X band (8.6 GHz), and was taken 8 November 2003.

## 3. DATA REDUCTION AND ANALYSIS

The HST data were obtained and underwent data reduction on June 9, 2008. The first step of the data reduction process was to run the program Multidrizzle to correct for telescope dithering and to reject cosmic rays. Multidrizzle is a program within pyraf, the python-based version of IRAF. Due to problems with the header files, the data reduction process took longer than expected. Ultimately, all exposures corresponding to a visit were drizzled over all four chips of WFPC-2 together by Multidrizzle to produce a total of six drizzled output files.

The IRAF task imcopy was used to cut a rectangular image of the target and some nearby objects out from the combined image that included all four WFPC-2 chips. The nearby objects would later be used as reference points. The six cut-out images were then shifted to a unified coordinated system using the IRAF task imshift. The nearby objects were used as reference points for the shift, with the IRAF task imexamine as the program to identify specific coordinates of the reference objects. Once the appropriate shifts were made to the corresponding images, the IRAF task imcombine was used to combine images based on what WF chip the target is located on for the visit. Therefore, the two drizzled images of visit 50 and 51 were combined, the two images of visit 60 and 61 were combined, and the two images of visit 70 and 71 were combined.

The polarization calibrator tool at the Space Telescope Sciences Institute website was then used to analyze the three images and obtain the I, Q, and U Stokes parameters for the three images. The inputs were the WFPC-2 chip used, the polarization filter, and PA V3. PA V3 was obtained from the image header file. Once the Stokes parameters were obtained, a pyraf script was used to obtain the polarization images: I Pol, Q Pol, and U Pol, also called the Stokes parameters.

In addition, the P and PA outputs were obtained from the script, as well as the associated error files for all output images. The custom pyraf script was written by Alex Padgett and used in Perlman et al. (2006). The script uses the polarization-calibration tool coefficients along with the three drizzled combined images of the source to produce the three polarization images; intensity, Q, and U. It also produces the fractional polarization image, the magnitude of polarization image, and the error images for all the output images.

Since this data has such high noise levels, Gaussian statistics cannot be used. This script utilizes Rician statistics to avoid this issue. Polarimetry data is inherently Rician in nature, but if the signal to noise ratio is very high, the Rician statistics error become equivalent to the Gaussian errors (citepepper06). Since the polarization is a positive definite quantity, the Gaussian distribution

is unreliable. The Q and U polarization images are used to find the RMS that is used in a second iteration of the script to adjust the errors properly. So, two iterations of this script are needed to get statistically correct data. This first run is to get the U and Q images to calculate the RMS (using the `imstat` task in AIPS), then the second run using the RMS to give statistically correct values for the fractional polarization image and its error image, as well as the magnitude polarization image and its error image.

Using the Stokes parameters from the I pol image and the following equations, we obtained P and PA:

$$P = \sqrt{U^2 + Q^2} \quad (1)$$

$$PA = \tan^{-1}\left(\frac{Q}{U}\right) \quad (2)$$

The polarization images block averaged two by two using `blkavg` in IRAF. To create the contour plot and X-ray images, the AIPS environment was used. The AIPS task `PCNTR` was used to make a contour image with polarization vectors of the target. The optical image was then overlaid with an X-ray image, and a radio image, using the AIPS tasks `hgeom` and `greys`. Contours of the optical image were included.

After all the steps of data reduction were completed, the analysis of the data began. It was clear that even after the initial step of data reduction, using `Multidrizzle`, that there was still a significant amount of noise left in the images. This is probably due to the difficulty of using `WFPC-2` instead of using `ACS`. With another run of `Multidrizzle`, a more grounded understanding of the statistics used in the raw data files, and with different parameter choices, the noise from these images may have been more successfully removed. It is not clear if this noise is due to cosmic rays, hot pixels, or a combination of the two. To make `Multidrizzle` run, the header files had to be edited to remove the second filter from the `IDCTAB`. It may be worth another iteration of reduction for future use of this data.

#### 4. RESULTS

In Figures 1-3, we show the jet of PKS 1136-135 in both polarized and total optical emission, as well as in the radio and X-rays. In Figure 1, we show the radio image of the jet overlaid on the HST Stokes I (total intensity) image. This shows the basic structure of the jet. As can be seen, it contains three main knots, called A, B, and C. The A knot is closest to the AGN, while knot C is the furthest. As can be seen, optical emission is detected for all three of these regions, as well as possibly another region closer to the nucleus. Point source subtraction could reveal the optical emission from this knot, but was not done because of the time constraints for this project. No optical emission is detected on the counterjet side, although some stars and/or companion galaxy are seen superposed on the radio lobe.

In Figure 2, we show the polarization in the optical image, with flux contours from the optical Stokes I map overlaid. In that plot, we do not show polarization vectors for objects fainter than 0.016 % of the peak flux, translating to only slightly fainter than knots A and B. The C knot could not be included because the contour

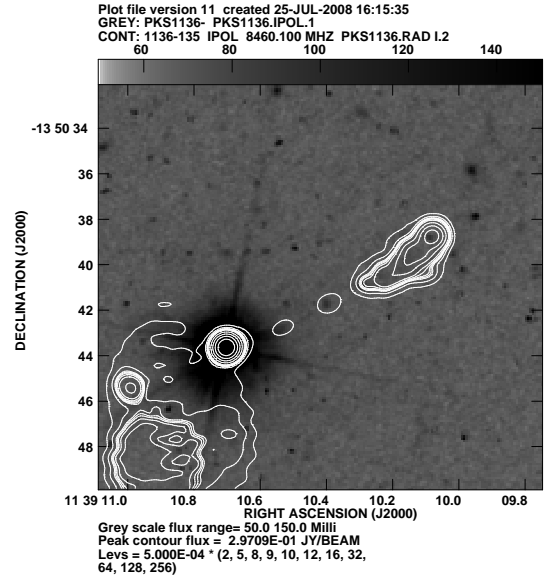


FIG. 1.— Optical grey scale image overlaid with radio contours of the three knots of PKS 1136-135. The magnitude of the contour levels is .0005. The levels of contour of the radio data is: 8, 9, 10, 12, 16, 32, 64, 128, 256

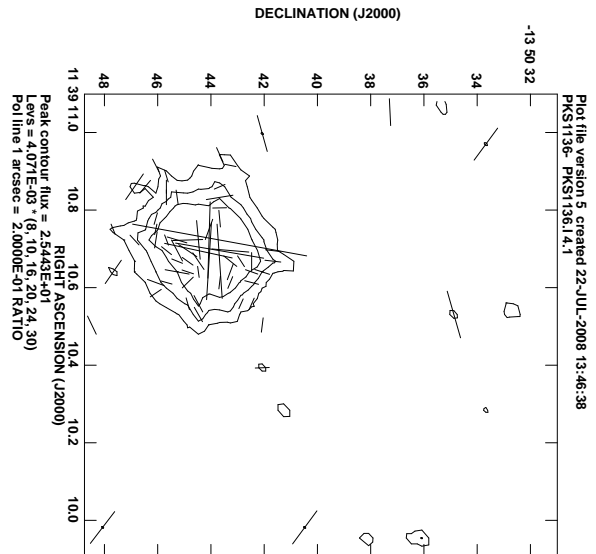


FIG. 2.— Contour of the AGN and two of the knots in the Jet structure along with polarization vectors. The percent level cut-off is .016; the value just below the intensity of the knots A and B.

level would have to be set too low. This would include too much noise to incorporate the C knot. The polarization cut-off was set to be just below the polarization value of the C knot in the polarization image. As can be seen, significant polarization is detected in knot A, but not in knot B.

To quantify this, we used the `DS9/SAOimage` program to conduct photometry on the output polarization files. Table 1 shows the results of the polarimetric analysis for the three main jet knots, giving fractional polarization and error for each, in percent. We detect a polarization of  $\sim 30\%$  in knot A, significant at the  $6\sigma$  level. However, in knots B and C we do not detect significant polarization, as the results are only at the 1-2  $\sigma$  level.

TABLE 1  
POLARIZATION OF JET COMPONENTS

Knot	Fractional Polarization	Percent error
A	32.7	5.5
B	7.0	4.8
C	5.9	5.2

Figure 3 shows the optical Stokes I image in greyscale, overlaid with contours taken from the *Chandra* X-ray image. As with the contour-polarization vector plot, the levels were chosen to show the AGN structure in the X-ray image as well as the structure of the two knots closest to the AGN.

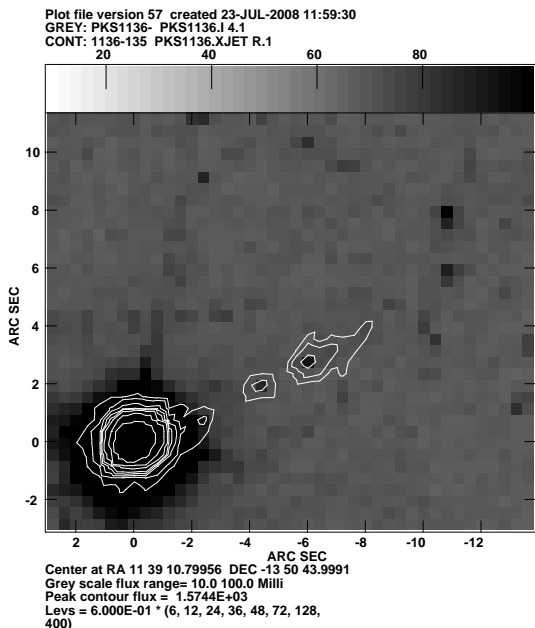


FIG. 3.— Optical grey scale image with X-ray contours of the closest two knots of pks1136-135. The magnitude of the contour levels is set to .06. The grey scale pixel range is set from .01 to .10. The levels of contour are: 4, 8, 12, 16, 32, 64, 128, 256

## 5. CONCLUSIONS

From the data analysis we can see that there is in fact a significant amount of polarization from the A knot. This would imply a synchrotron emission mechanism of some type. It is interesting that the other knots do not show significant polarization. For these knots the only possible emission mechanism is inverse-Compton scattered CMB emission. The lack of significant polarized emission in these regions rules out both the synchrotron as well as the SSC mechanism, which while energetically unfavorable (it requires the jet to be out of equipartition by orders of magnitude and viewed at a very specific angle) was still just barely viable based on previous data.

Thus, we see that in fact the jet of PKS 1136-135 is most likely a mixture of both inverse-Compton and synchrotron emission in the optical. This is a very interesting result as logical thought would suggest a ruling mechanism would like be dominant and not shared: Either one is synchrotron or one is inverse-Compton. This supports previous predicted models by Uchiyama that the A

knot is optically polarized and thus obeys a synchrotron model, while knot B does not fit the synchrotron model in the optical band, and is in fact obeying an inverse-Compton model.

## 6. FUTURE WORK

A future iteration of data reduction would be advantageous to refine the results obtained in this project. Specifically, the problem with cosmic rays should be addressed. Cosmic rays were very prevalent in nearly every exposure of the source. This coupled with a few more iterations of drizzling could lead to optical resolution of the relativistic jet, which was not resolvable at this time. As previously mentioned, this is the most precise observation ever taken of this object in the optical band, not just in the polarimetry realm, but also in the photometric as well.

A ultraviolet measurement of the polarization at knot A could explain if this feature is in fact itself polarized, or if the polarization is due to a residual effect not associated with the jet. This could tell us if in fact the emission mechanism is in fact inverse-Compton off of the Cosmic Microwave Background, or due to a self-Synchrotron Compton effect. Nevertheless, there is no instrument currently available that can achieve this. The closest instrument nearing production is the proposed Space Ultraviolet-Visible Observatory (SUVO) (Shull 2003). This would be cause for such an instrument to be built if equipped with the necessary polarization instrumentation.

The structure in the radio contour overlay with the intensity-polarization grey scale image discovered between the AGN incident to the knots of the jet would be an interesting feature to explore. Perhaps this is a part of the structure of the jet. A future point-source subtraction will help us resolve features blocked out by the nucleus. Point source subtraction could also be used for studying the scattered polarized light from the AGN itself.

Lastly, this project could aid in the understanding of these jet mechanisms on the larger scale. PKS 1136-135 could be used as a model for optical jets associated with quasars. Due to its relative proximity, when comparing to other quasars, higher resolution can be obtained on PKS 1136-135 than most other quasars. Understanding of how this object works could translate to most other quasars.

I would like to thank Professor Eric Perlman for support and advice with my project. I would like to thank the Southeastern Association for Research in Astronomy (SARA) for participation in their summer REU program. I would like to thank Max Mutchler of the Space Telescope Science Institute, Baltimore, MD, for aiding in the complex data reduction of this project. I would like to thank Alex Padgett of the University of Maryland, Baltimore County, for use of his custom pyraf script for data reduction. This project was funded by a partnership between the National Science Foundation (NSF AST-0552798), Research Experiences for Undergraduates (REU), and the Department of Defense (DoD) AS-SURE (Awards to Stimulate and Support Undergraduate Research Experience) programs.

## REFERENCES

- Harris, D. E., Krawczynski, H. 2006, ARAA, 44, 463.
- Jester, S., Harris, D. E., Marshall, H. L., Meisenheimer, K. 2006 ApJ, 648, 900
- Longair, Malcolm S. High Energy Astrophysics : Particles, Photons and Their Detection. New York: Cambridge UP, 1992.
- Longair, Malcolm S. High Energy Astrophysics Vol. 2 : Stars, the Galaxy and the Interstellar Medium. New York: Cambridge UP, 1994.
- Perlman, E. S., et al. 2006 ApJ, 651, 735
- Shull, J. M. 2003, Hubble's Science Legacy: Future Optical/Ultraviolet Astronomy from Space, 291, 17
- Sambruna, R. M., Maraschi, L., Tavecchio, F., Urry, C. M., Cheung, C. C., Chartas, G., Scarpa, R., & Gambill, J. K. 2002, ApJ, 571, 206.
- Uchiyama, Y., et al. 2007 ApJ, 661, 719